

## **General Disclaimer**

### **One or more of the Following Statements may affect this Document**

- This document has been reproduced from the best copy furnished by the organizational source. It is being released in the interest of making available as much information as possible.
- This document may contain data, which exceeds the sheet parameters. It was furnished in this condition by the organizational source and is the best copy available.
- This document may contain tone-on-tone or color graphs, charts and/or pictures, which have been reproduced in black and white.
- This document is paginated as submitted by the original source.
- Portions of this document are not fully legible due to the historical nature of some of the material. However, it is the best reproduction available from the original submission.

AD-A016 530

MEASUREMENT OF ENERGETIC PARTICLE RADIATION AT THE  
SYNCHRONOUS ALTITUDE ABOARD ATS-6

George A. Paulikas, et al

Aerospace Corporation

Prepared for:

Space and Missile Systems Organization  
National Aeronautics and Space Administration

30 September 1975

DISTRIBUTED BY:



National Technical Information Service  
U. S. DEPARTMENT OF COMMERCE

309123

REPORT SAMSO-TR-75-227

AD-A016530

# Measurement of Energetic Particle Radiation at the Synchronous Altitude Aboard ATS-6

G. A. PAULIKAS, J. B. BLAKE, and S. S. IMAMOTO  
Space Physics Laboratory  
Laboratory Operations  
The Aerospace Corporation  
El Segundo, Calif. 90245

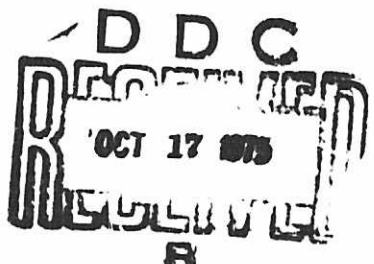
30 September 1975

Interim Report

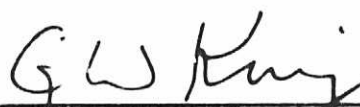
APPROVED FOR PUBLIC RELEASE:  
DISTRIBUTION UNLIMITED

Prepared by  
**SPACE AND MISSILE SYSTEMS ORGANIZATION**  
**AIR FORCE SYSTEMS COMMAND**  
Los Angeles Air Force Station  
P.O. Box 92960, Worldway Postal Center  
Los Angeles, Calif. 90009

Reproduced by  
**NATIONAL TECHNICAL  
INFORMATION SERVICE**  
U.S. Department of Commerce  
Springfield, VA 22151

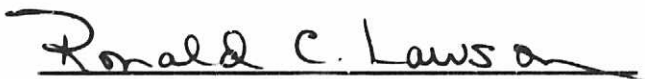


**Approved**

  
G. W. King  
G. W. King, Vice President and  
General Manager  
Laboratory Operations

This technical report has been reviewed and is approved for publication. Publication of this report does not constitute Air Force approval of the report's findings or conclusions. It is published only for the exchange and stimulation of ideas.

**FOR THE COMMANDER**

  
Ronald C. Lawson  
Ronald C. Lawson, 2nd Lt.  
United States Air Force  
Technology Development Division  
Deputy for Technology

ACCESSION for	
RTIS	<input checked="" type="checkbox"/> White Section
DIC	<input type="checkbox"/> Ref. Section
UNARMED	
JUSTIFICATION	
.....	
BY	
DISTRIBUTION/AVAILABILITY CODES	
Bloc.	AVAIL. AND OR SPECIAL
A	

## UNC LASSIFIED

SECURITY CLASSIFICATION OF THIS PAGE (When Data Entered)

REPORT DOCUMENTATION PAGE		READ INSTRUCTIONS BEFORE COMPLETING FORM
1. REPORT NUMBER SAMSO-TR-75-227	2. GOVT ACCESSION NO.	3. RECIPIENT'S CATALOG NUMBER
4. TITLE (and Subtitle) MEASUREMENT OF ENERGETIC PARTICLE RADIATION AT THE SYNCHRONOUS ALTITUDE ABOARD ATS-6		5. TYPE OF REPORT & PERIOD COVERED Interim
7. AUTHOR(s) George A. Paulikas, J. Bernard Blake, and Sam S. Imamoto		6. PERFORMING ORG. REPORT NUMBER TR-0076(6260-20)-7 8. CONTRACT OR GRANT NUMBER(s) F04701-75-C-0076
9. PERFORMING ORGANIZATION NAME AND ADDRESS The Aerospace Corporation E! Segundo, Calif. 90245		10. PROGRAM ELEMENT, PROJECT, TASK AREA & WORK UNIT NUMBERS
11. CONTROLLING OFFICE NAME AND ADDRESS Space and Missile Systems Organization Air Force Systems Command Los Angeles, Calif. 90045		12. REPORT DATE 30 September 1975
14. MONITORING AGENCY NAME & ADDRESS(if different from Controlling Office)		13. NUMBER OF PAGES 28 32
		15. SECURITY CLASS. (of this report) Unclassified
		15a. DECLASSIFICATION/DOWNGRADING SCHEDULE
16. DISTRIBUTION STATEMENT (of this Report)  Approved for public release; distribution unlimited.		
17. DISTRIBUTION STATEMENT (of the abstract entered in Block 20, if different from Report)		
18. SUPPLEMENTARY NOTES		
19. KEY WORDS (Continue on reverse side if necessary and identify by block number) Particle Environment Solar Pronons Synchronous Altitude Trapped Electrons Trapped Radiation		
20. ABSTRACT (Continue on reverse side if necessary and identify by block number) The Aerospace Corporation energetic electron-proton spectrometer operating on ATS-6 is described. This experiment detects energetic electrons in four channels between 140 keV and greater than 3.9 MeV, measures energetic protons in five energy channels between 2.3 and 80 MeV and energetic alpha particles in three channels between 9.4 and 94 MeV. After more than a year of operation in orbit, the experiment continues to return excellent data on the behavior of energetic magnetospheric electrons as well as information regarding the fluxes of solar protons and alpha particles.		

## PREFACE

This experiment was the product of a large number of people whose efforts spanned many years - not because the experiment is particularly complex but because the launch of ATS-F (now ATS-6) receded several times. We are particularly grateful to Mrs. G. Roberts for the mechanical design of the experiment, to the Westinghouse group, particularly Frank McNally, Joe Ramsey and Bill King, for their excellent support in the many test and checkout activities and to Bob Wales of GSFC and his associates who saw the experiment through from beginning to end. Paul McKowan of GSFC is providing excellent support in the data acquisition phase of this work. Mrs. Teri Becker wrote the data analysis program which we have used to date.

This work was supported primarily by the U. S. Air Force Space and Missiles Organization Contract F04701-74-C-0075 with Aerospace Corporation. Portions of the data analysis efforts were supported under NASA Contract NASW-2762.

## CONTENTS

PREFACE .....	1
I. INTRODUCTION .....	5
II. DESCRIPTION OF THE EXPERIMENT .....	7
A. Physical and Electronic Configuration .....	7
B. Detector Calibration Data .....	11
III. OPERATIONAL HISTORY .....	19
IV. PRELIMINARY RESULTS .....	21
A. Energetic Electrons .....	21
B. The Solar Proton Event of 4, 5, 6 July 1974 .....	24
V. SUMMARY .....	29
REFERENCES .....	31

**Preceding page blank**

## FIGURES

1.	Spatial relationships near the synchronous orbit at local midnight between the ring current, the plasmapause, the energetic particle trapping boundary and the earthward terminus of the plasma sheet .....	6
2.	Overall view of The Aerospace Corporation energies particle spectrometer on ATS-6 .....	8
3.	Schematic block diagram of detector/electronic system .....	9
4.	Efficiency of detection of electrons in the E1 channel .....	12
5.	Effective area of the E2, E3 and E4 electron channels as a function of electron energy .....	13
6.	Efficiency for detection of protons in the P1 and P2 channels of the counter telescope .....	16
7.	Comparison of energetic electron count-rates observed by ATS-6 and ATS-1 during a magnetically quiet day .....	22
8.	Comparison of energetic electron count rates observed by ATS-6 and ATS-1 during a magnetically disturbed day .....	23
9.	Count rates of proton and alpha channels of Aerospace Corp. experiment during the solar proton event of July 1974 .....	26
10.	Increase in solar proton flux associated with a sudden commencement near 15:35 on 4 July 1974 .....	27

## I. INTRODUCTION

The region of space near the synchronous altitude is a fascinating region of space where various domains of the magnetosphere meet and interact. Figure 1, taken from the work of Frank (1971), graphically illustrates the confluence of the plasmapause, the extra-terrestrial ring current, the boundary of the zone of energetic particles and the earthward terminus of the plasma sheet in the immediate vicinity of  $6.6 R_e$ . The study of the interaction of the various plasmas with vastly different densities and temperatures and the energization and dynamics of these plasmas are the goals of the Environmental Measurements Experiments (EME) on ATS-6.

The Aerospace experiment described in this paper contributes to these goals through measurements of the high energy tail of the electron distribution function. Our experiment covers the energy range, for electrons, from 140 keV to greater than 3.9 MeV, and we expect our experiment to yield important results regarding the acceleration and dynamics of the energetic electrons. While previous measurements (see the compilations by *...e and Incero (1967)*, and *Singley and Vette (1972)*) have contributed a great deal of information regarding the behavior of energetic electrons at the synchronous altitude, comprehensive measurements, such as those being made on ATS-6 of the entire distribution function for a given particle species has never been made.

Not shown in Fig. 1, but also present in this region of space during solar particle events, are energetic protons and alpha particles (and possible electrons) of solar origin. These solar particles may penetrate to altitudes as low as  $4 R_e$  (depending on particle rigidity and magnetic activity) but, in general, the gradient of solar protons is located somewhere in the vicinity of  $6.6 R_e$ . The Aerospace experiment measures the fluxes and spectra of solar particles reaching the synchronous orbit. (The proton thresholds of this experiment are too high to permit the detection of the proton component of the trapped radiation.)

The sections below describe the instrumentation in some detail and provide examples of results obtained during the first year of the operation of ATS-6.

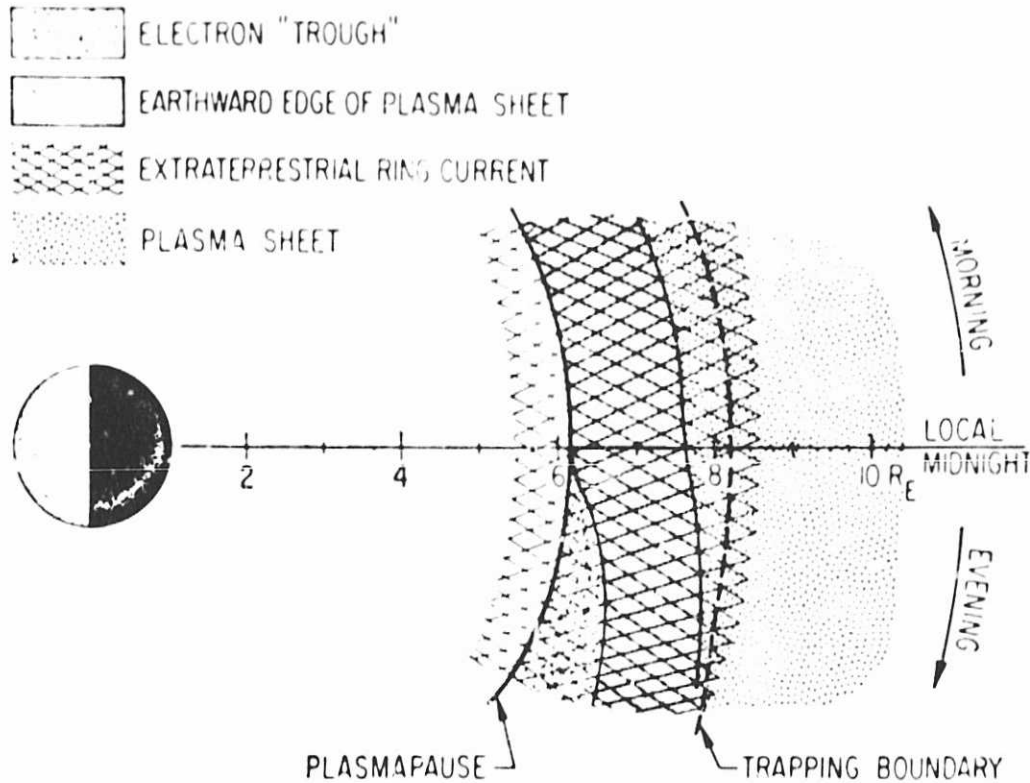


Fig. 1. Spatial relationships near the synchronous orbit at local midnight between the ring current, the plasmapause, the energetic particle trapping boundary and the earthward terminus of the plasma sheet. This figure is qualitative and representative of magnetic quiet (from Frank, 1971).

## II. DESCRIPTION OF THE EXPERIMENT

### A. Physical and Electronic Configuration

The instrument consists of four separate sensors, one two detector element telescope and three omnidirectional single detector units. An overall view of the instrument is presented in Figure 2; a functional schematic of the electronics is presented in Figure 3.

The counter telescope uses silicon surface-barrier detectors of ORTEC manufacture behind a disc-loaded collimator. The first detector is a  $50 \text{ mm}^2$  area,  $230\mu$  deep device and the second has a  $200 \text{ mm}^2$  area and is  $100\mu$  deep. Both are totally depleted. Five electronic discriminator levels are used with the first detector. The two upper levels are set above the maximum energy a proton can deposit in the detector and thus are sensitive to alphas only (actually  $Z \geq 2$ ). The next two levels are sensitive to protons (actually all ions) but not electrons and the lowest level is sensitive to all particles in the appropriate energy range. The sole function of the second detector is to inhibit from analysis any penetrating particles. Section B provides details about the energy channels.

The three omnidirectional sensors use small cubical lithium-drifted silicon detectors, manufactured by SSR, centered under a hemispherical shell and heavily shielded (relative to the hemispherical shield) over the rear  $2\pi$  solid angle. Protons are separated unambiguously from electrons by setting the second discriminator level well above the maximum energy an electron can deposit in the small semiconductor detector. The fact that  $dE/dx$  (energy loss per unit path length) is much greater for protons than for electrons (in the energy range of geophysical interest) is utilized. The absence of electron contamination in the proton channels was verified by electron irradiation of the sensors. The proton threshold of each of the three sensors was determined primarily by the thickness of the hemispherical shield, with the energy threshold of the two most lightly shielded units somewhat affected by the electronic thresholds as well. The most lightly shielded omnidirectional sensor has a third electronic level set above the maximum proton energy

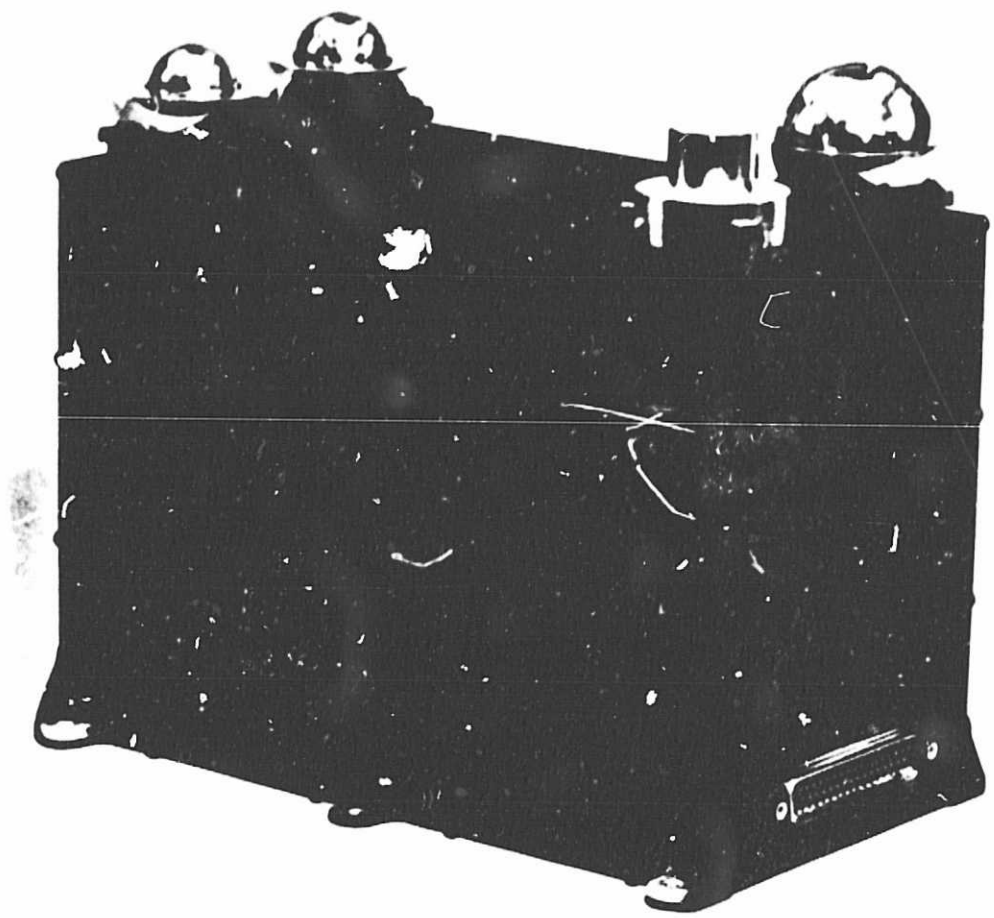


Fig. 2. Overall view of The Aerospace Corporation energies particle spectrometer on ATS-6. Omnidirectional detectors are housed inside the cylindrical collimator structure in the foreground.

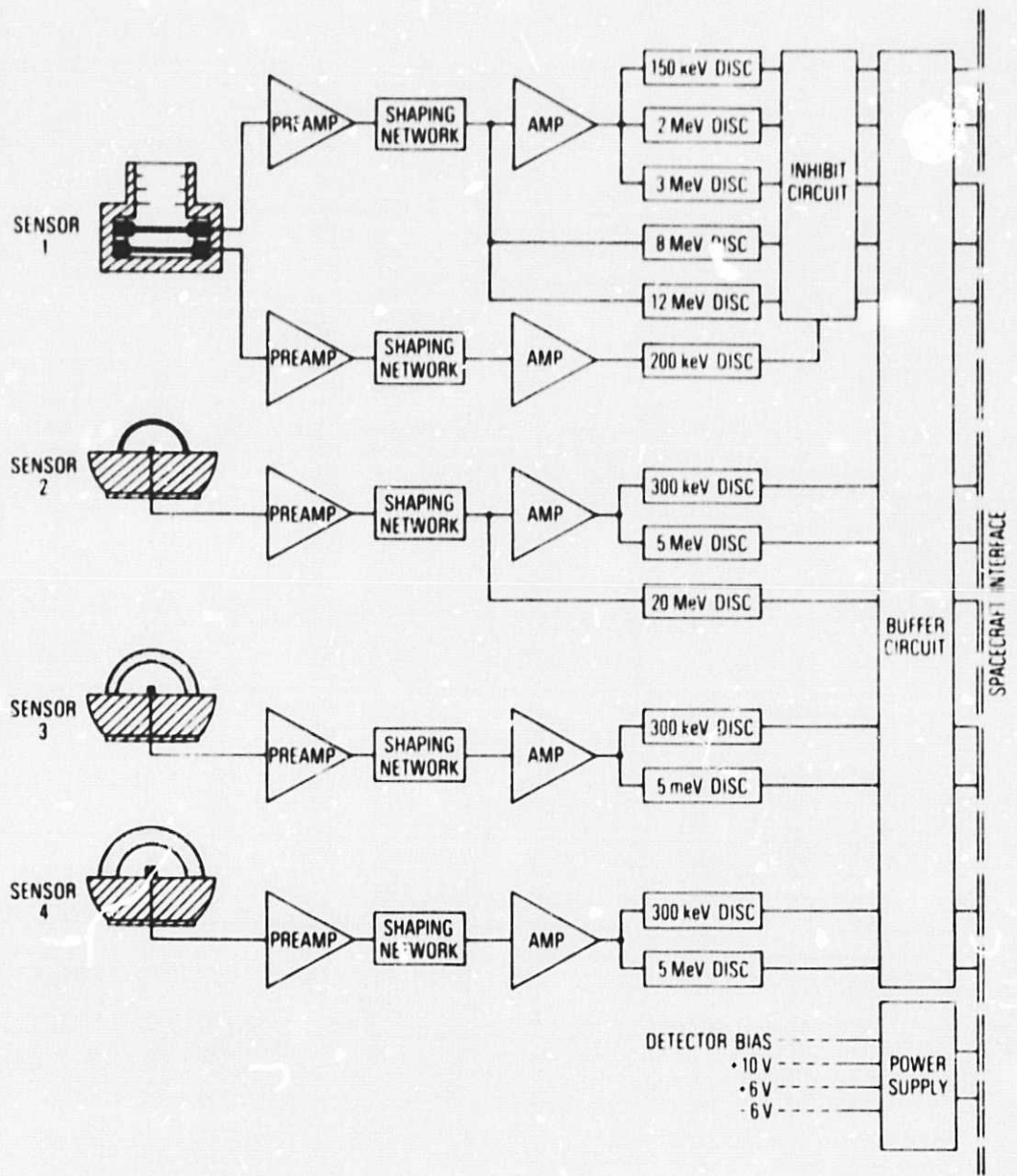


Fig. 3. Schematic block diagram of detector/electronic system.

deposit to provide an alpha particle channel. The two heavier hemispherical shields were made of beryllium to minimize bremsstrahlung and maximize the threshold sharpness. The most lightly shielded shield is aluminum since an aluminum shield is much cheaper and the performance difference negligible for such a thin shield.

The electronic sub-system of the experiment are shown schematically in Figure 3. The input stage of the pre-amps utilize an n-channel field-effect-transistor. In order to maintain a low system noise, the input stage is enclosed in a shielded compartment. The characteristic long-tail pulse from the pre-amp is shaped by a pole-zero shaping network into a pulse with a 1 microsecond time constant. The high level discriminators (>8 MeV) are driven directly from the output of the shaping circuit. Output from the shaping network is also coupled to an operational amplifier which provides the additional gain required to trigger the low energy thresholds. Pre-amp gain is set by an adjustable feedback capacitor. Gain of the op-amp is set by a feedback resistor.

The discriminator is essentially a comparator driving a tunnel diode. The threshold voltage is set by a lab-set resistor. Output from the discriminator is 0-5 volts pulse with an approximate duration of a microsecond. A COS/MOS buffer circuit accepts the 0-5 volts discriminator pulse and provides a 0-10 volt pulse to interface with the spacecraft encoder.

Sensor 1 uses two sets of circuits identical to those used for Sensors 2, 3 and 4. The front detector of the two detector array has five discriminators which drive an inhibit circuit; particles penetrating through the first detector are thus rejected. COS/MOS logic is used to perform the trailing edge logic in the inhibit circuit. Trailing edge logic is used to compensate for "walk" in the discriminators. Outputs from the inhibit circuit are also buffered to interface with the encoder.

A DC-DC converter provides the required instrument bias voltages. Power from the spacecraft is coupled to a series pass stage to limit the experiment turn-on transient and protect spacecraft relays. The converter section is completely enclosed in an electrostatic shield to minimize undesirable pickup by the counting circuits. Total power consumption is 475-540 milliwatts, depending on the count rate at which the instrument is operating.

Terminal boards with discrete components and point to point wiring are used in the construction of the amplifiers, discriminators and power supply. Printed circuit and integrated circuits are used for the inhibit and buffer circuits. Total experiment weight is 2.6 pounds.

#### B. Detector Calibration Data

##### 1. Electron Channels

Figures 4 and 5 display the electron calibration data in graphical form. The E1 channel employed a directional geometry of  $1.6 \times 10^{-1} \text{ cm}^2\text{-sr}$ , the E2, E3 and E4 channels used an omnidirectional geometry and thus the calibration data, obtained with a plane parallel beam, must be integrated over the angular acceptance of these detectors in order to arrive at the omnidirectional efficiency as a function of energy. However, it is convenient to define thresholds and geometric factors for obtaining rapid estimates of fluxes. These thresholds and geometric factors are calculated by numerically integrating the response function over various spectral shapes and finding the threshold which minimizes the variation of the calculated geometric with spectral shape. The results are given in Table 1.

The proton and alpha particle channels have negligible sensitivity to electrons.

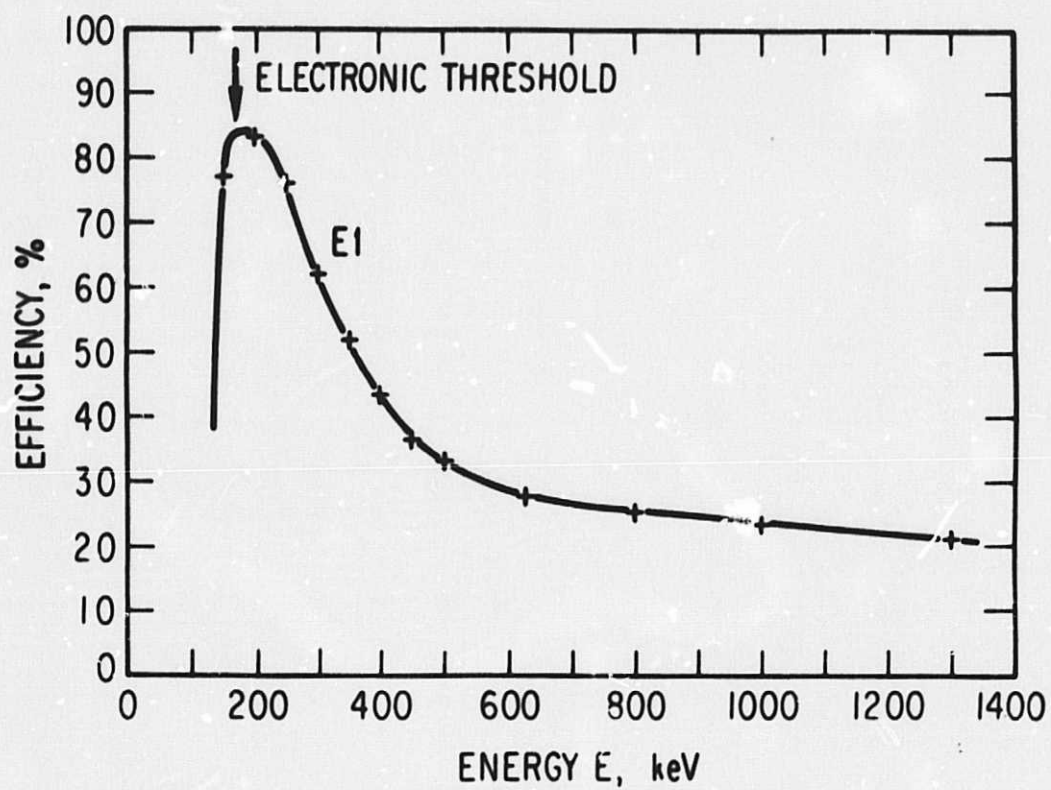


**Fig. 4.** Efficiency of detection of electrons in the E1 channel. This channel has a nominal energy sensitivity of 140-600 keV. Sensitivity of this channel below the nominal electronic threshold is associated with the finite noise of the detector.

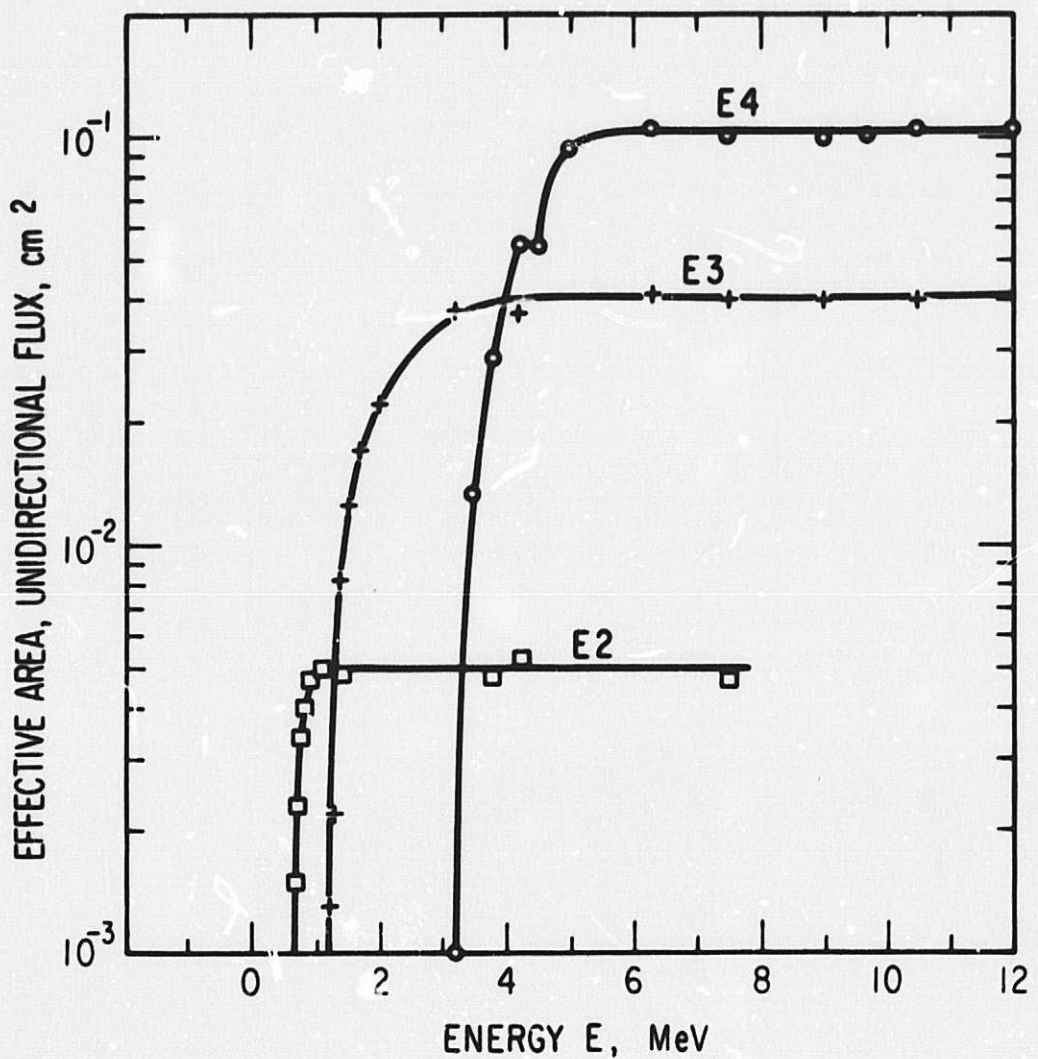


Fig. 5. Effective area of the E2, E3 and E4 electron channels as a function of electron energy. This effective area, when integrated over the angular response of the detector, yields the omnidirectional geometric factor.

TABLE I.

Channel	Passband or Threshold (MeV)	$\epsilon G$
E1	0.140 - 0.600	.115 cm <sup>2</sup> - sr
E2	0.700	.00349 cm <sup>2</sup>
E3	1.55	.0176 cm <sup>2</sup>
E4	3.90	.0688 cm <sup>2</sup>

## 2. Proton Channels

The proton calibration data for channels P1 and P2 are shown in Figure 6. The thresholds of these two channels are sharp enough [ $\Delta E/E_{\text{threshold}} \ll 1$  where  $\Delta E \sim E (\epsilon = 90\%) - E (\epsilon = 10\%)$ ] to eliminate the need for numerically integrating over the response function. The geometric factors of the other proton channels (the omnidirectional sensors) were computed, and spot-checked at several energies where accelerator protons were available. Table 2 gives the results. Unfortunately, ATS-6 weight constraints prevented the use of sufficient back shielding to render back penetration negligible for all proton spectra. Two different thicknesses of shielding covered the rear hemisphere and thus each channel has three passbands and geometric factors. These "rear passbands" are also given in Table 2.

In all cases the electron channels are sensitive to protons. However, as a general rule, at the synchronous orbit the electron fluxes far exceed those of the trapped protons. Under unusual conditions, i.e., during solar proton events apparent electron counts can be due to protons. The efficiencies of the electron channels for protons are given in Table 3.

The proton channels can be triggered by alphas (or higher Z); the relative abundance of alphas to protons renders this contamination negligible.

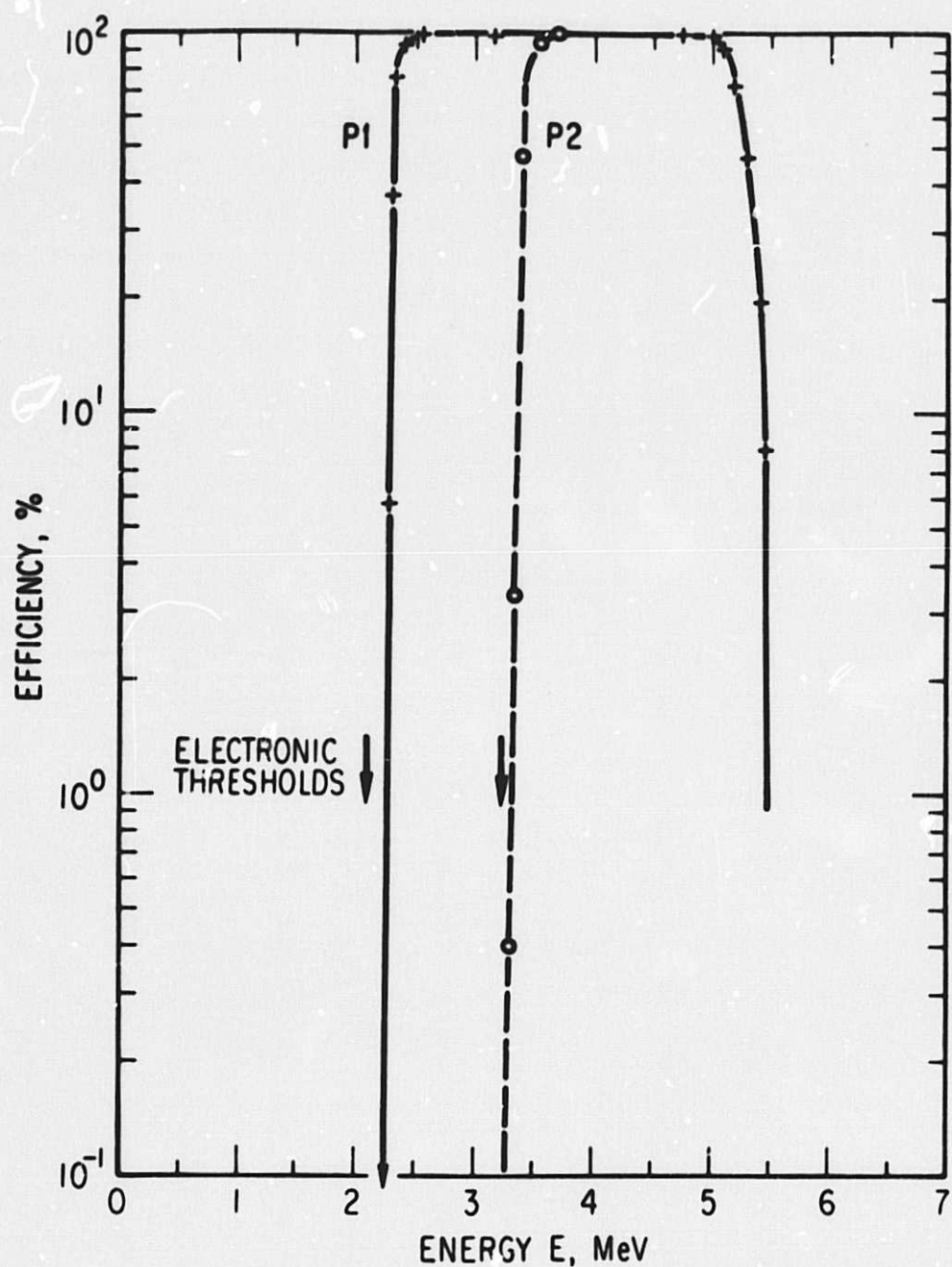


Fig. 6. Efficiency for detection of protons in the P1 and P2 channels of the counter telescope.

TABLE 2.

Channel	Energy (MeV)	G	Particle
P1	2.3-5.3	.160 cm <sup>2</sup> - sr	p
P2	3.4-5.3	.160 cm <sup>2</sup> - sr	p
P3	9.4-21.2	.160 cm <sup>2</sup> - sr	$\alpha$
P8	13.4-21.2	.160 cm <sup>2</sup> - sr	$\alpha$
P4	12-26	.0045 cm <sup>2</sup>	p
P5	46-100	.0048 cm <sup>2</sup>	$\alpha$
P6	20-52	.0188 cm <sup>2</sup>	p
P7	40-90	.0412 cm <sup>2</sup>	p
<u>Rear Passbands</u>			
P4a	58-68	.0023 cm <sup>2</sup>	p
P4b	85-96	.0017 cm <sup>2</sup>	p
P5a	232-265	.0033 cm <sup>2</sup>	$\alpha$
P5b	344-370	.0031 cm <sup>2</sup>	$\alpha$
P6a	58-86	.0135 cm <sup>2</sup>	p
P6b	86-109	.0128 cm <sup>2</sup>	p
P7a	58-108	.0368 cm <sup>2</sup>	p
P7b	86-132	.0318 cm <sup>2</sup>	p

TABLE 3.

Channel	Energy (MeV)	G	Particle
E1	* see footnote	.16 cm <sup>2</sup> - sr	p
E2	12-190	.0074 cm <sup>2</sup>	p
E3	21-290	.0287 cm <sup>2</sup>	p
E4	40-520	.0617 cm <sup>2</sup>	p
<u>Rear Passbands</u>			
E2a	58-310	.0061 cm <sup>2</sup>	p
E2b	86-330	.0057 cm <sup>2</sup>	p
E3a	58-470	.0260 cm <sup>2</sup>	p
E3b	86-490	.0244 cm <sup>2</sup>	p
E4a	58-550	.0595 cm <sup>2</sup>	p
E4b	86-650	.0565 cm <sup>2</sup>	p

\*The E1 electron channel is sensitive to protons with energies greater than 710 keV. The upper limit of sensitivity is of the order 190 MeV without the veto trigger, about 5.3 MeV when the particle enters, in such a way as to hit the veto detector.

### **III. OPERATIONAL HISTORY**

The Aerospace experiment on ATS-6 was first powered in orbit on 14 June 1974. The experiment has been operating almost continuously since that time; such brief shutdowns of the experiment as have occurred have been associated with tests of other experiments on ATS-6. Several minor anomalies in the performance of the experiment have been observed during the first year of operation; none of these affect the quality of utility of the data in any significant way and we consider that all goals of the experiment are being met.

#### IV. PRELIMINARY RESULTS

In this section we present a brief summary of the preliminary results already obtained from our ATS-6 experiment. These summaries are indications of some of the unique contributions ATS-6 data will make to our understanding of the behavior of the magnetosphere and the entry and motion of solar particles in the magnetosphere.

##### A. Energetic Electrons

When the first data on energetic electrons obtained by ATS-6 was examined, we noticed that the electron fluxes were much more dynamic than earlier observations (Paulikas et al., 1968; 1969; 1971) on ATS-1 had indicated. ATS-6 data indicated the virtual disappearance of energetic electrons during portions of the orbit in the night-time quadrant. Such "dropouts" were observed only rarely on ATS-1. In order to make a quantitative check on this impression, we obtained data from our experiment from ATS for the same time period and have made a direct comparison of ATS-6 and ATS-1 energetic electron observations. These comparisons are illustrated in Figures 7 and 8. Figure 7 illustrates observations made during a magnetically quiet period (Day 201) which was preceded by three days of magnetic quiet. In general, ATS-6 and ATS-1 energetic electron count-rates show similar behavior. The sharp decreases in flux near 0430 UT and 0630 UT visible in the ATS-6 data are the results of substorms. Note that the effects of substorm on the energetic electrons are much attenuated at ATS-1 as compared to ATS-6.

We find that during geomagnetically active periods, there is a very substantial difference in the count-rates observed by the two spacecraft. Figure 8 illustrates a comparison of observations made at ATS-6 and ATS-1 during a disturbed period. Note the total disappearance of flux at ATS-6 while ATS-1 always observes finite fluxes.

Preceding page blank

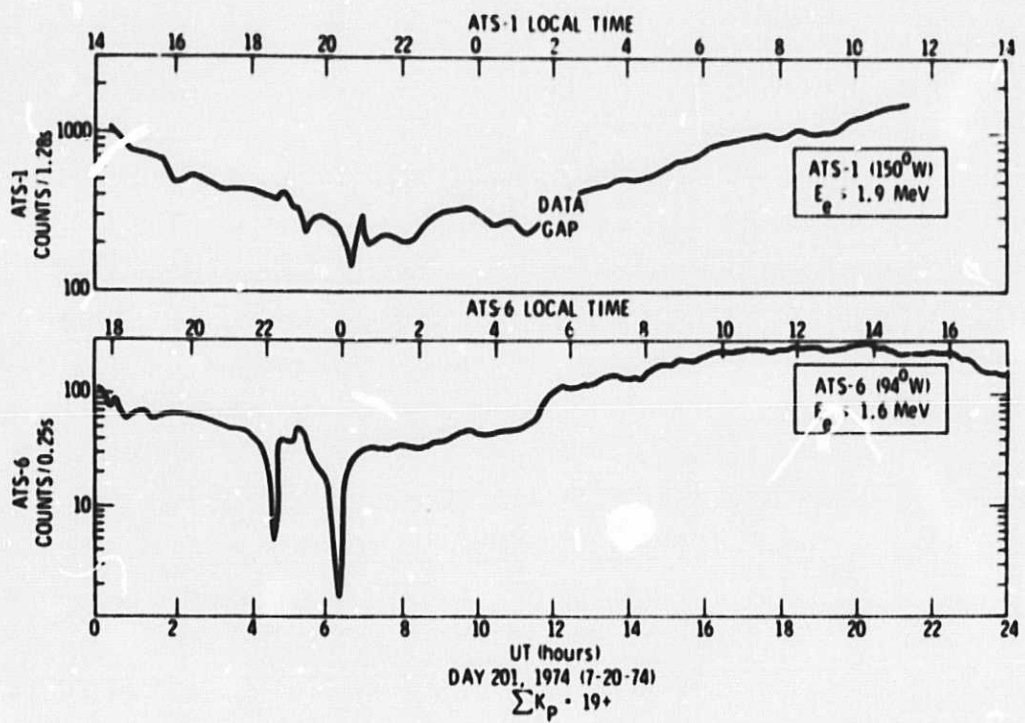
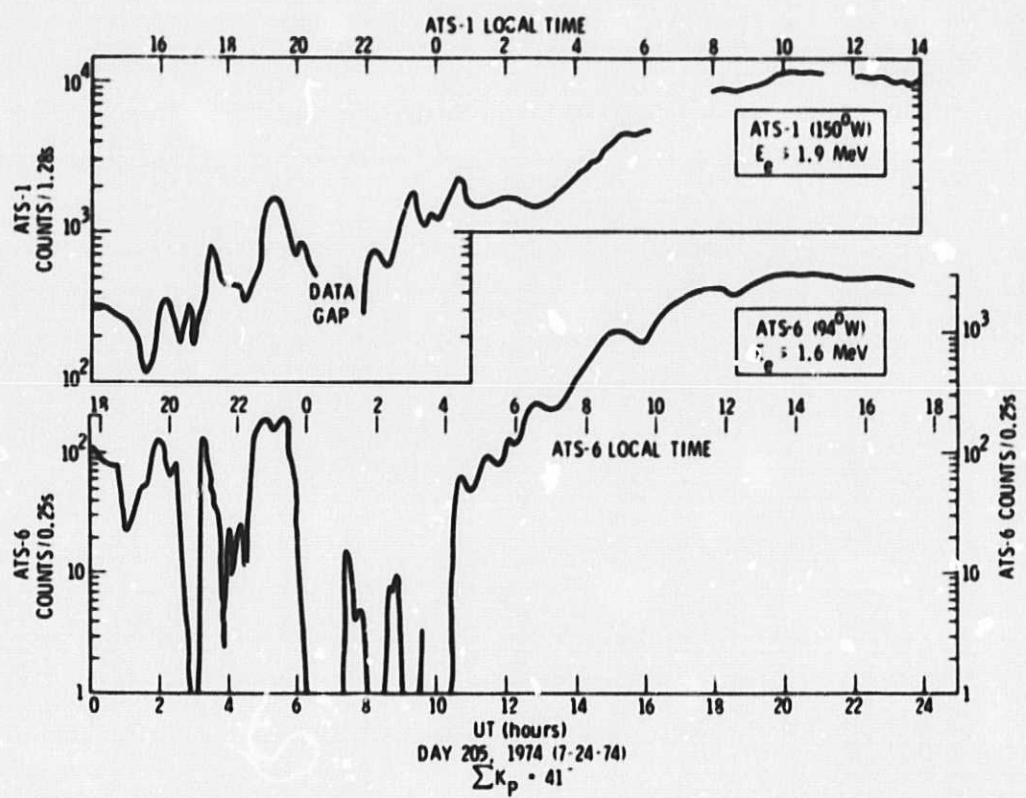


Fig. 7. Comparison of energetic electron count-rates observed by ATS-6 and ATS-1 during a magnetically quiet day (Day 201). The three days preceding Day 201 were also quiet.



**Fig. 8. Comparison of energetic electron count rates observed by ATS-6 and ATS-1 during a magnetically disturbed day (Day 205).**

The differences in phenomenology appear to be due to the different magnetic latitudes of the spacecraft. ATS-6 is located at about  $10^{\circ}$  magnetic latitude at its location of  $94^{\circ}$  W longitude, while ATS-1 is almost exactly on the magnetic equator at  $150^{\circ}$  W. The  $\sim 10^{\circ}$  difference in magnetic latitude appears to be sufficient to place ATS-6, at times, into regions of space devoid of energetic electrons. Substorms, for example, as illustrated in Figure 7, have a greater effect on the energetic particle population off the magnetic equator. We can postulate that, during the later stages of a substorm, the geomagnetic field relaxes to more dipole-like configuration and the boundary of energetic particle trapping moves inward and equatorward past the ATS-6 spacecraft.

The comparisons of ATS-6 data with ATS-1, while still preliminary, indicate a surprisingly steep gradient in the energetic electron population as one moves away from the equator, in other words, a disk-like region of trapping of energetic electrons near  $6.6 R_e$ .

#### B. The Solar Proton Event of 4, 5, 6 July 1974

Several solar proton events have been observed by the ATS-6 detectors during the first year of operation. Although at the present time we are at a relatively quiescent state of the cycle of solar activity, modest outburst of protons (and heavy nuclei) were emitted by the sun during July and September of 1974 and detected by the Aerospace experiment and other experiments aboard ATS-6.

Solar protons of even relatively low energy are able to reach the synchronous altitude quite readily, without very much decrease in the flux as these particles transverse the outer regions of the geomagnetic field. This surprising result was first noted by experiments on ATS-1 (Lanzerotti, 1968; Paulikas and Blake, 1969). The ATS-6 experiments will provide very much better insight regarding the trajectories by which solar particles penetrate deeply into the magnetosphere, the gradients of solar particle fluxes near the synchronous orbits and the effects of electromagnetic waves on the motion and lifetime of solar particles inside the geomagnetic cavity.

An overall view of the July, 1974 solar proton event, as observed by The Aerospace Corp. experiment on ATS-6, is presented in Figure 9. The entire event is quite complex. The complexity arises partly because several emission of particles by the sun, somewhat separated in time, are superimposed and partly because disturbances in the geomagnetic field were also affecting the fluxes of solar particles.

The effect of one such disturbance, a compression of the geomagnetic field (presumably by an interplanetary shock) on solar protons moving within the geomagnetic field, is illustrated in Figure 10. The effect of such a compression is to increase the observed flux within a given energy channel because particles are accelerated. The acceleration process is identical to that which operates in betatrons. Furthermore, the changes in the configuration of the geomagnetic field causes the particle flux gradient to move past the detector. Study of the time development of flux changes, such as illustrated in Figure 10, can give information regarding the way particles interact with the spectrum at electromagnetic waves created during geomagnetic activity (Paulikas and Blake, 1970).

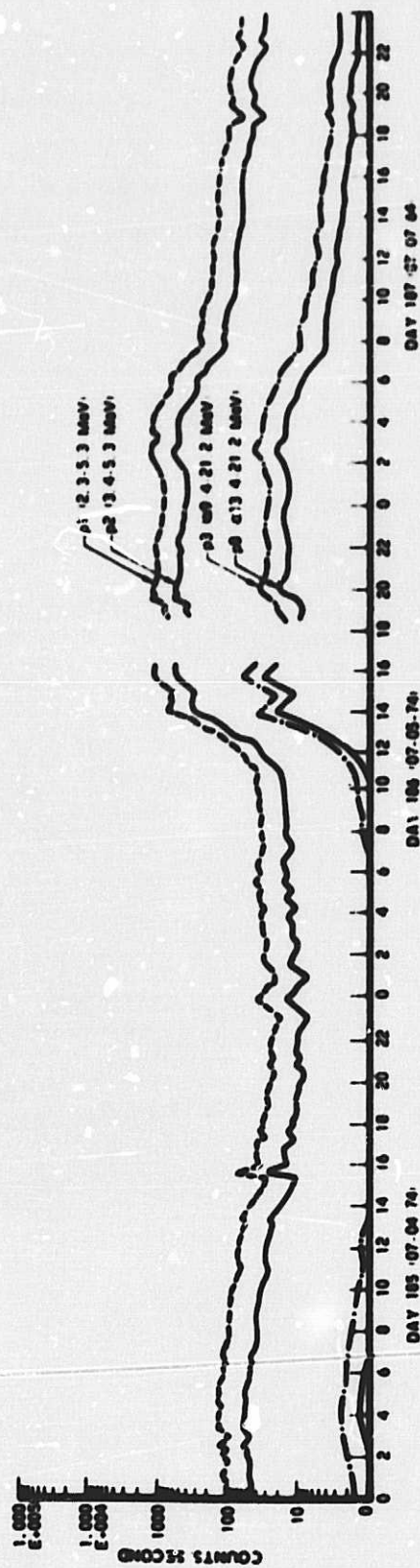
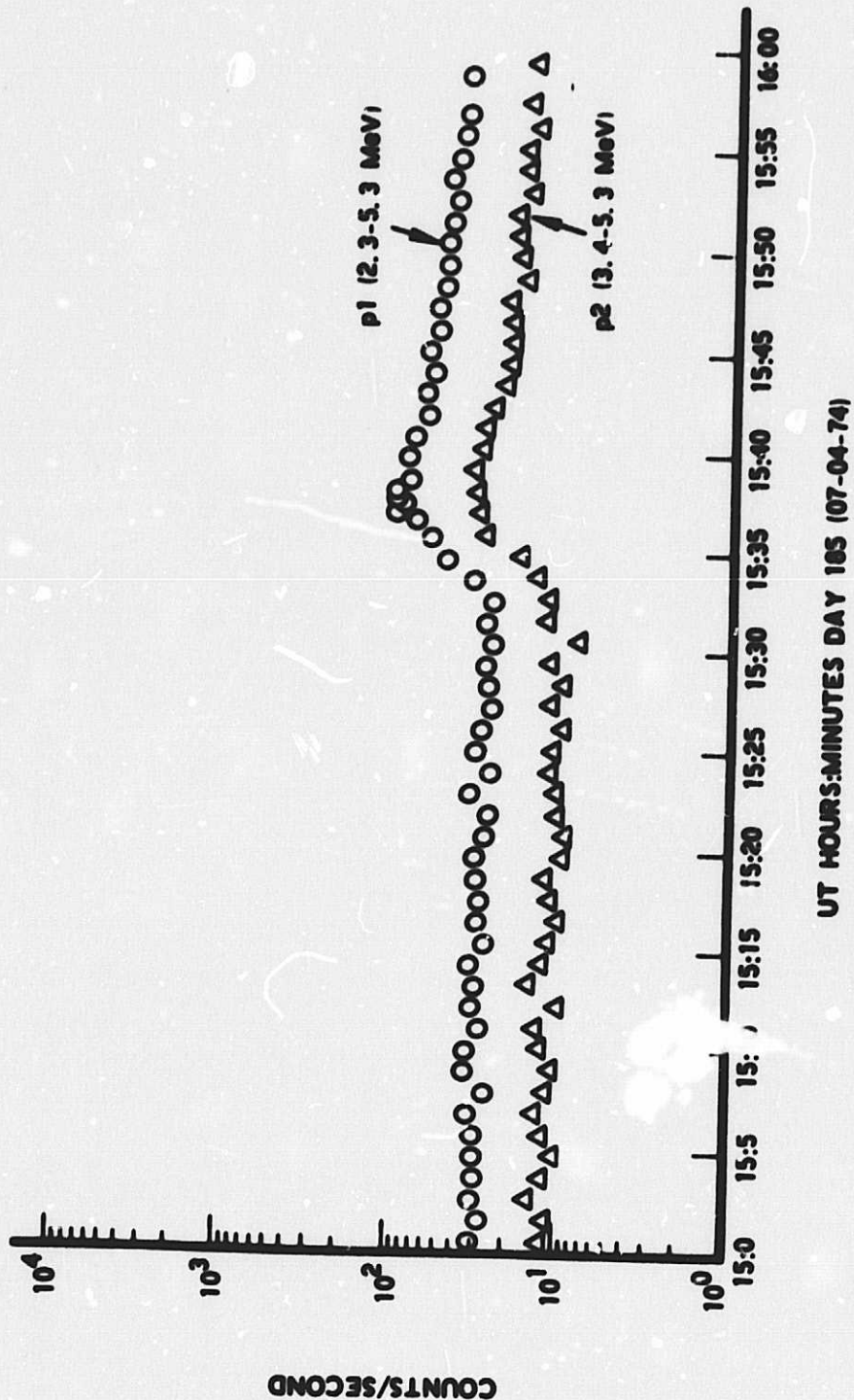


Fig. 9. Count rates of proton and alpha channels of Aerospace Corp. experiment during the solar proton event of July 1974. Data for two proton channels and two alpha channels for 4, 5 and 6 July 1974 are presented here.



V. SUMMARY

After more than a year of operation in orbit, the Aerospace Corporation experiment continues to provide excellent data. All design goals of the experiment have been met. While data analysis is still in the preliminary stages, it is clear that our experiment on ATS-6 will provide new and unique data regarding the behavior of energetic electrons at the synchronous altitude. In particular, correlation of ATS-6 data with data from other synchronous orbit spacecraft now operating (ATS-1, ATS-5) or planned for the future launches (GEOS) will give a much more complete view of the magnetospheric processes operating at high altitudes.

Preceding page blank

## REFERENCES

- Frank, L. A., "Relationships of the Plasma Sheet, Ring Current, Trapping Boundary and Plasmapause Near the Magnetic Equator and Local Midnight," *J. Geophys. Res.* 76, 2265 (1971).
- Lanzerotti, L., "Penetration of Solar Protons and Alphas to the Geomagnetic Equator," *Phys. Rev. Lett.*, 21, 929 (1968).
- Paulikas, G. A. and Blake, J. B., "Effects of Sudden Commencements on Solar Protons at the Synchronous Altitude," *J. Geophys. Res.* 75, 734 (1970).
- Paulikas, G. A. and Blake, J. B., "Penetration of Solar Protons to Synchronous Altitude," *J. Geophy. Res.* 74, 2161 (1969).
- Paulikas, G. A. and Blake, J. B., "The Particle Environment at the Synchronous Altitude. Models of the Trapped Radiation Environment, Vol. VII. Long Term Variations," NASA SP-3024 (1971).
- Paulikas, G. A., Blake, J. B., Freden, S. C., and Imamoto, S. S., "Observations of Energetic Electrons at Synchronous Altitude, I. General Features and Diurnal Variations," *J. Geophys. Res.* 73, 4915 (1968).
- Paulikas, G. A., Blake, J. B. and Palmer, J. A., "Energetic Electrons at the Synchronous Altitude: A Compilation of Data," Aerospace Corporation report No. TR-0066(5260-20)-4 (November 1969).
- Singley, G. W., and J. I. Vette, "A Model Environment for Outer Zone Electrons, NSSDC 72-13, (December 1972).
- Vette, J. I. and Lucero, A. B., "Models of the Trapped Radiation Environment, Volume III, Electrons at Synchronous Altitudes," NASA SP-3024 (1967).

Preceding page blank

## LABORATORY OPERATIONS

The Laboratory Operations of The Aerospace Corporation is conducting experimental and theoretical investigations necessary for the evaluation and application of scientific advances to new military concepts and systems. Versatility and flexibility have been developed to a high degree by the laboratory personnel in dealing with the many problems encountered in the nation's rapidly developing space and missile systems. Expertise in the latest scientific development is vital to the accomplishment of tasks related to these problems. The laboratories that contribute to this research are:

Aerophysics Laboratory: Launch and reentry aerodynamics, heat transfer, reentry physics, chemical kinetics, structural mechanics, flight dynamics, atmospheric pollution, and high-power gas lasers.

Chemistry and Physics Laboratory: Atmospheric reactions and atmospheric optics; chemical reactions in polluted atmospheres; chemical reactions of excited species in rocket plumes; chemical thermodynamics, plasma and laser-induced reactions; laser chemistry, propulsion chemistry, space vacuum and radiation effects on materials, lubrication and surface phenomena, photo-sensitive materials and sensors, high precision laser ranging, and the application of physics and chemistry to problems of law enforcement and biomedicine.

Electronics Research Laboratory: Electromagnetic theory, devices, and propagation phenomena, including plasma electromagnetics; quantum electronics, lasers, and electro-optics; communication sciences, applied electronics, semiconducting, superconducting, and crystal device physics, optical and acoustical imaging; atmospheric pollution; millimeter wave and far-infrared technology.

Materials Sciences Laboratory: Development of new materials; metal matrix composites and new forms of carbon; test and evaluation of graphite and ceramics in reentry; spacecraft materials and electronic components in nuclear weapons environment; application of fracture mechanics to stress corrosion and fatigue-induced fractures in structural metals.

Space Physics Laboratory: Atmospheric and ionospheric physics, radiation from the atmosphere, density and composition of the atmosphere, auroras and airglow; magnetospheric physics, cosmic rays, generation and propagation of plasma waves in the magnetosphere; solar physics, studies of solar magnetic fields; space astronomy, x-ray astronomy; the effects of nuclear explosions, magnetic storms, and solar activity on the earth's atmosphere, ionosphere, and magnetosphere; the effects of optical, electromagnetic, and particulate radiations in space on space systems.

THE AEROSPACE CORPORATION  
El Segundo, California